

Published in final edited form as:

J Neurosci. 2009 May 20; 29(20): 6394–6405. doi:10.1523/JNEUROSCI.4909-08.2009.

Mitochondrial Cholesterol Loading Exacerbates Amyloid Beta Peptide-Induced Inflammation and Neurotoxicity

Anna Fernández, Laura Llacuna, José C. Fernández-Checa¹, and Anna Colell.¹

Department of Cell Death and Proliferation, Institut d'Investigacions Biomèdiques de Barcelona, Consejo Superior de Investigaciones Científicas and Liver Unit, Hospital Clinic i Provincial, Centro de Investigaciones Biomédicas Esther Koplowitz, and CIBEREHD, IDIBAPS, 08036-Barcelona, Spain

Abstract

The role of cholesterol in Alzheimer's disease has been linked to the generation of toxic amyloid β peptides ($A\beta$). Using genetic mouse models of cholesterol loading, we examined whether mitochondrial cholesterol regulates $A\beta$ neurotoxicity and AD pathology. Isolated mitochondria from brain or cortical neurons of transgenic mice overexpressing SREBP-2 (sterol regulatory element binding protein 2) or NPC1 (Niemann-Pick type C1) knockout mice exhibited mitochondrial cholesterol accumulation, mitochondrial GSH (mGSH) depletion and increased susceptibility to $A\beta$ 1-42-induced oxidative stress and release of apoptogenic proteins. Similar findings were observed in pharmacologically GSH-restricted rat brain mitochondria, while selective mGSH depletion sensitized human neuronal and glial cell lines to $A\beta$ 1-42-mediated cell death. Intracerebroventricular human $A\beta$ delivery co-localized with mitochondria resulting in oxidative stress, neuroinflammation and neuronal damage that were enhanced in Tg-SREBP-2 mice and prevented upon mGSH recovery by GSH ethyl ester co-infusion, with a similar protection observed by i.p. administration of GSH ethyl ester. Finally, APP/PS1 mice, a transgenic AD mouse model, exhibited mitochondrial cholesterol loading and mGSH depletion. Thus, mitochondrial cholesterol accumulation emerges as a novel pathogenic factor in AD by modulating $A\beta$ toxicity via mGSH regulation; strategies boosting the particular pool of mGSH may be of relevance to slow down disease progression.

Keywords

Amyloid beta; cholesterol; mitochondrial oxidative stress; mitochondrial glutathione; $A\beta$ icv infusion; neuroinflammation

Introduction

Alzheimer's disease (AD) is a major neurodegenerative disorder characterized by progressive memory loss and cognitive impairment due to neuronal death mainly in cortex and hippocampus (Mattson, 2004; Zlokovic, 2005; Selkoe, 2007). Given the lack of effective therapy and its association with aging, AD is one of the most pressing health challenges worldwide. Although AD pathogenesis is still unknown, accumulation or faulty brain clearance of neurotoxic amyloid β peptides ($A\beta$) is thought to play a key role in AD (Walsh and Selkoe, 2004; Tanzi et al., 2004; Haass and Selkoe, 2007; Deane and Selkoe, 2007). Indeed, recent

Corresponding author: Anna Colell, Dept. Cell Death and Proliferation. Institut d'Investigacions Biomèdiques de Barcelona (IIBB-CSIC). Rosselló 161, 08036-Barcelona, Spain. Phone: (34) 93 363 8310; Fax: (34) 93 363 8301; E-mail: anna.colell@iibb.csic.es, or Jose C Fernandez-Checa, checa229@yahoo.com.

¹Anna Colell and José C. Fernández-Checa share senior authorship.

data have showed that A β dimers isolated directly from AD brains impair synaptic plasticity and memory (Shankar et al., 2008).

In addition to aging, epidemiological observations identified hypercholesterolemia in mid-life as a major risk factor for AD (Notkola et al., 1998; Anstey et al., 2008; Wolozin et al., 2000). Despite that studies examining statin usage have produced mixed conclusions, the epidemiological evidence linking cholesterol to AD has been supported by *in vivo* (Shönknecht et al., 2002; Bandaru et al., 2007) and *in vitro* studies (Fassbender et al., 2001; Kalvodova et al., 2005; Osenkowski et al., 2008), indicating that membrane cholesterol promotes the amyloidogenic processing of the membrane bound amyloid precursor protein (APP) by the β -secretase BACE1 (beta-site APP-cleaving enzyme 1) and γ -secretase to generate toxic A β .

Well before plaques are observed, intracellular aggregates of A β develop early in AD transgenic mice, which congregate in synaptic compartments and correlate with cognitive impairment (Oddo et al., 2003). Current evidence indicates the targeting of A β to intracellular sites, most notably mitochondria, causing oxidative stress, mitochondrial dysfunction and cell death (Manczak et al., 2006; Caspersen et al., 2005; Lin and Beal, 2006; Lustbader et al., 2004; Casley et al., 2002).

Mitochondria do not synthesize GSH *de novo* and mitochondrial GSH (mGSH) originates by the transport of cytosol GSH into mitochondria by a specific carrier whose sensitivity to changes in membrane fluidity has been previously characterized (reviewed in Fernandez-Checa and Kaplowitz, 2005). Cholesterol-mediated changes in membrane dynamics impairs the mitochondrial transport of GSH, resulting in the depletion of mGSH, a critical antioxidant defense that determines the susceptibility to stimuli that induce mitochondrial oxidative stress, such as TNF- α , Fas or hypoxia (Mari et al., 2006; Colell et al., 1997; Mari et al., 2008; Lluís et al., 2006). However, the specific role of mGSH in the regulation of A β toxicity has not been previously described. Thus, we addressed whether mitochondrial cholesterol accumulation modulates A β neurotoxicity and AD pathology, using genetic models of cholesterol loading, namely, transgenic mice overexpressing SREBP-2 and NPC1^{-/-} mice (Yu et al., 2005). Overall, these findings expand the role of cholesterol in AD, indicating that in addition to fostering A β production, mitochondrial cholesterol loading determines A β neurotoxicity and AD-like pathology via mGSH depletion. Although total GSH depletion and altered GSH redox cycle have been described in AD (Resende et al., 2008; Boyd-Kimball et al., 2005), the fact that the pool of mGSH rather than cytosol GSH determines A β susceptibility implies that efforts should be directed to specifically replenish mGSH to slow down disease progression, using strategies that bypass the block of GSH transport into mitochondria imposed by cholesterol deposition.

Materials and Methods

Tg-SREBP-2, NPC1^{-/-} and Tg-APP/PS1 mice

Breeding pairs of B6;SJL-Tg(rPEPCKSREBF2)788Reh/J, BALB/cJ NPC1^{NIH} and B6C3-Tg (APP^{swe},PSEN1^{dE9})85Dbo/J mice were obtained from The Jackson Laboratory (Bar Harbor, MA). At the time of weaning (21 days), mice were genetically identified by PCR using DNA prepared from tail-tips and following the genotyping protocols provided by the supplier. All procedures involving animals and their care were approved by the ethics committee of the University of Barcelona and were conducted in accordance with institutional guidelines in compliance with national and international laws and policies.

Cell cultures

SH-SY5Y human neuroblastoma (ECACC) and C6 rat glioma cell lines were grown in Ham's F12 (Sigma) containing 10% FBS and 2 mM glutamine. U118 human glioma and neuroglioma

H4 cell lines were maintained in DMEM medium (Invitrogen) supplemented with 10% FBS and 2 mM glutamine. Mice neuron-rich cultures were obtained from the cerebral cortex of embryos (day 16) using standard techniques. Dissociated cells were suspended in Neurobasal™ medium (Invitrogen) with 2.5% (v/v) B27 supplement (Invitrogen), 0.5 mM glutamine, and 10% FBS and plated onto poly-D-lysine coated plates at a cell density of $2 \times 10^5 / \text{cm}^2$. The culture medium was changed 3 h after plating and every other day thereafter. After 24 h *in vitro*, the culture medium was replaced with serum-free medium. Experiments were performed at 6 d *in vitro* (DIV). The cellular composition of the cultures was evaluated at this time by immunohistochemical analysis using antibodies to neuron- and glial-specific markers and was found to consist of >95% neurons.

Mitochondrial isolation

Cerebral cortices were isolated and homogenized in 210 mM Mannitol, 60 mM Sucrose, 10 mM KCl, 10 mM Sodium succinate, 1mM ADP, 0.25 mM DTT, 0.1 mM EGTA, 10 mM HEPES, pH 7.4. The homogenates were centrifuged at 600 g for 10 min, with the resulting supernatant being centrifuged at 10,300 g for 15 min. The resulting pellet was suspended in 2 ml, loaded onto 8 ml of 30% (v/v) Percoll gradient and centrifuged at 95,000 g for 30 min. The mitochondrial pellet was then rinsed twice by centrifuging 15 min at 7,000 g. Cortical neurons were fractionated into cytosol and mitochondria by digitonin permeabilization followed by oil gradient centrifugation as described previously in detail (Fernandez-Checa et al., 1987).

GSH and cholesterol measurements

GSH levels in homogenates or cytosol and mitochondria were analyzed by the recycling method (Tietze, 1969). For total cholesterol determination, 10 mg of protein was saponified with alcoholic KOH in a 60°C heating block for 30 min. After the mixture had cooled, 10 ml of hexane and 3 ml of distilled water were added and shaken to ensure complete mixing. Appropriate aliquots of the hexane layer were evaporated under nitrogen and used for cholesterol measurement. HPLC analysis was made using a Waters μ Bondapak C18 10- μ m reversed-phase column (30 cm \times 4 mm inner diameter), with the mobile phase being 2-propanol/acetonitrile (50:50, v/v) and the flow rate of 1 ml/min. The amount of cholesterol was calculated from standard curves and the identity of the peaks was confirmed by spiking the sample with known standards.

Preparation of A β peptides

Human recombinant A β 1-42 and A β 42-1 peptides (Bachem) were dissolved to 1 mM in hexafluoroisopropanol (HFIP) and aliquoted into microcentrifuge tubes, then the HFIP was evaporated, and the peptides were stored at 20°C until use. For oligomeric assembly, concentrated peptides were resuspended in DMSO (5 mM) and then diluted to 100 μ M in phenol red-free media and incubated at 4°C for 24 h. Western blot analysis demonstrated the presence of soluble oligomeric forms of A β (Supplemental Fig. S1).

A β infusion

The infusion model was adopted from previous work on the rat infusion model (Frautschy et al., 1996). Briefly, stainless steel cannula attached to micro-osmotic pumps (model #1004, Alzet) were stereotaxically implanted into the right lateral cerebral ventricle (at coordinates -1.0mm mediolateral and -0.5mm anterioposterior from Bregma; -2mm dorsal-ventral from skull). Pumps contained either oligomeric human A β 1-42 (0.45 μ g / μ l) in vehicle (4 mM HEPES pH 8.0 + 0.21 μ g / μ l of human high-density lipoprotein, HDL) or vehicle alone. HDL was used in the pump to reduce A β aggregation and enhance neuropil delivery. The pump contents were released over a period of 28 days at a rate of ~0.11 μ l / h (50 ng / h A β ; 26 ng / h HDL), which corresponds to 36 pmol / g brain / h. ELISA analyses indicated that the human

recombinant A β content found in the brain after this infusion period was 4.3 ± 0.6 ng / g, which is in the range of the levels found in transgenic mice and humans (Hsiao et al., 1996; Pirttila et al., 1997). At post-operative day 28, mice were anaesthetized and perfused with PBS buffer containing a protease inhibitor cocktail. The brains were then removed and longitudinally bisected. The right half of the brain was fixed and embedded for histological examination, while the left hemisphere was snap frozen for biochemical evaluation. Levels of endogenous or human recombinant A β 1-42 peptide in brain extracts were determined with duplicate measurements by the A β 1-42 ELISA kits from Biosource International, according to the manufacturer's instructions. In some cases, GSH ethyl ester was either added to the infusion solution (0.5 mmol / ml) as described before (Zeevalk et al., 2007), or injected i.p. (1.25 mmol / kg / day) every 12 hours over the last two weeks of the infusion period as described (Martensson et al., 1993) to test its efficacy in the protection against A β -mediated neuroinflammation and injury.

Immunohistochemistry

Cryopreserved sections (10 μ m) from -1.2 mm through -2.4 mm from Bregma were processed according to the avidin–biotin–peroxidase (ABC, Vectastain; Vector Lab.) staining method. After antigen retrieval treatment, the endogenous peroxidase was blocked by exposure to 2% H₂O₂ in methanol for 30 min. The sections were treated with the Avidin/Biotin blocking kit from Vector Lab according to the manufacturer's instructions. The primary antibodies: mouse anti-A β (1:300, Sigma), rabbit anti-GFAP (1:500, Dako) and rat anti-F4/80 (1:200, Santa Cruz Biotech.) were incubated overnight at 4°C. After washing with PBS, sections were then incubated for 1 h with appropriated biotinylated secondary antibodies at a dilution of 1:400, followed by ABC staining for 1 h. The immunoreaction was visualized with diaminobenzidine (DAB enhanced liquid substrate system, Sigma). Sections were counterstained with hematoxylin (Dako).

Immunofluorescence and laser confocal imaging

Cortical neurons were fixed for 15 min with 3.7% paraformaldehyde before permeabilization with 0.1% saponin in blocking buffer (1% BSA + 20 mM Glycine in PBS) for 15 min. Then, cells were incubated in the presence of anti-cytochrome c monoclonal antibody (1:200, clone 6H2.B4; PharMingen) diluted in blocking buffer with 0.025% saponin for 1 h at 37°C following 45 min incubation with the secondary antibody, FITC-conjugated goat anti-mouse IgG (1:400, Caltag Lab.). Filipin (50 mg/ml, Sigma) was added during the secondary antibody incubation. Dewaxed hippocampal sections were first boiled in citrate buffer (10 mM sodium citrate pH 6.0) and incubated with 0.1 M glycine / PBS for 20 min to reduce autofluorescence. Tissues processed for A β staining were pretreated with 99% formic acid for 7 min. The sections were incubated overnight at 4°C with monoclonal anti-A β 1-42 (1:300, Sigma) rabbit anti-cytochrome c (1:100, Santa Cruz Biotech), rat anti-F4/80 (1:200, Santa Cruz Biotech) and rabbit anti-GFAP (1:500, Dako) antibodies diluted in Antibody Diluent with Background Reducing Components from Dako. After washing in PBS, the sections were incubated for 45 min with the secondary antibodies diluted in the same vehicle solution. The secondary antibodies used were: FITC-conjugated goat anti-mouse IgG (1:400, Caltag Lab.), Cy3-conjugated anti-rabbit IgG, (1:400, Jackson ImmunoResearch Inc.) and Cy3-conjugated anti-rat IgG (1:400, Jackson ImmunoResearch Inc.). In some cases, nuclei were stained with Hoechst 33258 (2 μ g / ml) before mounting the samples in Fluoromount-G (Southern Biotech). Confocal images were collected using a Leica SP2 laser scanning confocal microscope equipped with UV excitation, an argon laser, a 633/1.32 OIL PH3 CS objective and a confocal pinhole set at 1 Airy unit. All the confocal images shown were single optical sections.

Caspase-3 activity and mitochondrial membrane potential ($\Delta\Psi_m$)

Caspase activation in cell extracts was determined spectrofluorometrically using the specific fluorescent substrate Ac-DEVD-AMC (100 μ M, Bachem). The release of 7-amino-4-trifluoromethyl coumarin (AMC) was continuously recorded with excitation at 355 nm and emission at 460 nm. The mitochondrial membrane potential was measured using tetramethylrhodamine ethyl ester (TMRE, 50 nM). The dye retention was analyzed with a Becton-Dickinson FACScan flow cytometer in FL2.

Electron microscopy

Pellets containing the mitochondria purified fraction were fixed in 3% glutaraldehyde, 10 mM sodium phosphate buffer, pH 7.2, post-fixed in 1% osmium tetroxide, dehydrated in graded steps of ethanol through propylene oxide, and embedded in Spurr (Sigma). Finally, ultra-thin sections were stained with uranyl acetate and lead citrate and photographed in a JEOL JEM 1010 electron microscope.

Statics

Results are expressed as means \pm SD. Statistical significance was performed using an analysis of variance (ANOVA) followed by Dunnett's post hoc tests for multiple comparisons or by the unpaired two-tailed Student's t test as indicated in the figure legends. A $P < 0.05$ value was considered statistically significant.

Results

Tg-SREBP-2 mice exhibit brain mitochondrial cholesterol accumulation, mGSH depletion and enhanced susceptibility to A β neurotoxicity

To examine whether brain mitochondrial cholesterol modulates A β toxicity we used transgenic mice overexpressing the truncated active form of the transcription factor SREBP-2 (Tg-SREBP-2), which controls cholesterol synthesis (Horton et al., 2002). We first assessed whether Tg-SREBP-2 mice displays the cholesterol accumulation in brain which has been reported in liver and adipose tissue (Horton et al., 1998). The quality of brain mitochondria from Tg-SREBP-2 mice was assessed by electron microscopy, and lack of contamination from endoplasmic reticulum, plasma membrane and endosomes was estimated from western blot analysis of PERK, Na⁺/K⁺ ATPase α 1, and Rab5A, respectively (Supplemental Fig. S2). Biochemical analyses indicated enhanced cholesterol levels in the homogenate and mitochondrial fraction of Tg-SREBP-2 mice with respect to wild type mice (Fig. 1A). mGSH is a critical mitochondrial antioxidant, which is negatively regulated by cholesterol accumulation due to impaired transport of cytosol GSH into mitochondria via modulation of membrane dynamics (Mari et al., 2006; Colell et al., 1997). Mitochondria from Tg-SREBP-2 mice exhibited lower mGSH levels compared to wild type mice, whereas the content of GSH in the homogenate remained unaffected (Fig. 1A). Next, we evaluated the mitochondrial response to A β -mediated oxidative stress. Soluble oligomeric A β 1-42 (1 μ M for 2 h) induced a ~2-fold higher DCF (2',7'-dichlorodihydrofluorescein) fluorescence, reflecting ROS generation in mitochondria from Tg-SREBP-2 mice compared to wild type mice (Fig. 1B), which was accompanied by enhanced release of cytochrome c and Smac/DIABLO (Fig. 1C). To further assess whether the increased sensitivity of isolated mitochondria to A β -induced oxidative stress impacts on neuronal death, we isolated cortical neurons from wild type and Tg-SREBP-2 embryos followed by A β exposure. Immunostaining analyses using the neuronal marker microtubule-associated protein 2 (MAP-2) confirmed the neuronal-enrichment of the cultures (Supplemental Fig. S3). Laser confocal microscopy indicated higher cholesterol levels in cortical neurons from Tg-SREBP-2 mice compared to wild type mice revealed by staining with filipin, a fluorescent polyene antibiotic that binds specifically to the 3 β -hydroxyl group

of sterols (Mari et al., 2006; Norman et al., 1972), which extensively co-localized with mitochondria stained with cytochrome c antibody (Fig. 1D). These findings were accompanied by lower GSH levels in mitochondria isolated from cortical neurons of Tg-SREBP-2 mice compared to wild type mice (2.1 ± 0.4 vs. 3.3 ± 0.5 nmol/mg prot.), with the sparing of cytosol GSH content (not shown). Finally, cortical neurons from Tg-SREBP-2 mice exhibited enhanced susceptibility to A β 1-42 (0.5 nM - 1 μ M for 48 h) mediated cell death compared to that of wild type mice (Fig. 1E). Importantly, this sensitivity in Tg-SREBP-2 mice is observed at a concentration of A β 1-42 as low as 5 nM.

Sensitivity of brain mitochondria from NPC1^{-/-} mice to A β -induced oxidative stress and release of proapoptotic proteins

NPC1 is a late endosomal protein involved in the intracellular transport of cholesterol, whose ablation results in cholesterol and sphingolipids loading and progressive neurodegeneration (Paul et al., 2004). Recently, elevated mitochondrial cholesterol levels and mitochondrial dysfunction has been reported in the liver (Mari et al., 2006) and brain (Yu et al., 2005) from NPC1^{-/-} mice. Cholesterol content was higher in brain mitochondria from NPC1^{-/-} mice compared to wild type mice (Fig. 2A), which was accompanied by 50-60% depletion of mGSH stores (Fig. 2A), without changes in cytosol GSH (not shown). To examine the susceptibility of brain mitochondria from NPC1^{-/-} mice to oligomeric A β , we first determined the generation of mitochondrial ROS following exposure to A β 1-42 (1 μ M for 2 h). As seen, DCF fluorescence in response to A β was higher in brain mitochondria from NPC1^{-/-} mice compared to mitochondria from NPC1^{+/+} brain (Fig. 2B). Moreover, A β incubation induced an enhanced release of cytochrome c and Smac/DIABLO in mitochondria from NPC1^{-/-} mice (Fig. 2C). Collectively the preceding findings in Tg-SREBP-2 and NPC1^{-/-} mice reveal the correlation between mitochondrial cholesterol loading and susceptibility to A β -induced oxidative stress and neurotoxicity, effects that are accompanied by selective mGSH depletion.

mGSH-dependent susceptibility of brain mitochondria to A β toxicity

Early GSH depletion and altered GSH redox cycle have been recently shown in AD transgenic mice (Resende et al., 2008). Although GSH levels protect against A β neurotoxicity and A β has been shown to stimulate ROS generation from mitochondria (Lin and Beal, 2006; Boyd-Kimball et al., 2005; Cardoso et al., 2001), however, the particular role of mGSH depletion on A β -mediated toxicity has not been specifically addressed before. To investigate this question, mitochondria from rat brain were depleted of GSH by ethacrynic acid (EA), which covalently binds to GSH. As shown, EA (5 μ M for 15 min) depleted mGSH levels (Fig. 3A) and enhanced DCF fluorescence by A β 1-42, indicative of higher ROS generation (Fig. 3B), an effect not observed when mitochondria were exposed to the non-toxic peptide A β 42-1 (Fig. 3B). A step-wise increase in mitochondrial DCF fluorescence by A β 1-42 peptide was observed as a function of mGSH depletion by EA, that was accompanied by enhanced mitochondrial lipid peroxidation, estimated from the fluorescence loss of cis-parinaric-stained mitochondria (Supplemental Fig. S4A-C). To rule out non-specific effects of EA, we depleted mGSH *in vivo* using buthionine sulfoximine (BSO), a specific inhibitor of γ -GCS (γ -glutamylcysteine synthetase), the rate-limiting enzyme in GSH biosynthesis (Jain et al., 1991). Brain mitochondria from BSO-treated rats exhibited mGSH depletion (Fig. 3A), recapitulating the effects observed with EA on A β -induced ROS generation (Fig. 3B). In addition, mGSH depletion by both strategies enhanced the mitochondrial release of cytochrome c (Fig. 3C) and Smac/DIABLO (not shown) after exposure to A β . To further analyze the source of ROS induced by A β , mitochondrial electron flow was blocked at different respiratory complexes (Fig. 3D). Inhibition of complex III by antimycin A potentiated ROS generation by A β in GSH-depleted mitochondria, while preincubation with rotenone and TTFA (thenoyltrifluoroacetone), which block complex I and II, respectively, prevented the A β -mediated increase of DCF fluorescence, pointing to complex III as the major site of ROS

generation by A β . These findings indicate that mGSH controls the mitochondrial oxidative stress generation by A β .

Selective mGSH depletion with the spare of cytosol GSH sensitizes human neuronal and glial cells to A β neurotoxicity

We next asked whether selective mGSH depletion modulates A β neurotoxicity. To address this question, human neuroblastoma SH-SY5Y cells were exposed to 3-hydroxy-4-pentenoate (HP), a fatty acid derivative which is biotransformed in mitochondria into a Michael electrophile and then conjugated with GSH, resulting in its depletion (Mari et al., 2006; Mari et al., 2008; Garcia-Ruiz et al., 2003). As seen, HP decreased mGSH levels with the sparing of GSH cytosol stores (Fig. 4A), sensitizing SH-SY5Y cells to A β -induced cell death (Fig. 4B). Similar results were observed in glial-derived H4, C6 and U118 cell lines following selective mGSH depletion by HP and A β challenge (Supplemental Fig. S5A, B), indicating that the role of mGSH in regulating A β cytotoxicity is not restricted to neuronal cells. mGSH depletion in SH-SY6Y cells by HP potentiated A β -induced DCF fluorescence, indicative of enhanced ROS generation, and loss of mitochondrial membrane potential (Supplemental Fig. S6A, B). Dying SH-SY5Y cells following HP plus A β exposure exhibited apoptotic features, including chromatin condensation/nuclear fragmentation (Fig. 4C) and increased caspase-3 activity (Fig. 4D). Interestingly, preincubation with the pancaspase inhibitor qVD-OPH (quinoline-Val-Asp-CH₂-difluorophenoxy) prevented the morphological changes in chromatin condensation (Fig. 4C) and caspase-3 activation (Fig. 4D) induced by HP plus A β challenge, but failed to protect against cell death (Fig. 4E). Pretreatment with antioxidants such as N-acetyl-cysteine (NAC) and butylated hydroxyanisole (BHA) significantly decreased ROS generation induced by HP plus A β exposure (Fig. 4F) and the combined pretreatment with NAC and qVD-OPH protected mGSH-depleted SH-SY5Y cells against cell death triggered by A β (Fig. 4E). Overall, these findings indicate that selective mGSH depletion sensitizes neuronal and glial cells to A β by stimulating oxidant-dependent cell death and caspase-independent apoptosis.

Neuroinflammation in Tg-SREBP-2 mice following in vivo infusion of human A β

Having shown that brain mitochondrial cholesterol modulates A β toxicity by regulating mGSH, we next evaluated the onset of pathological features of AD such as neuroinflammation following intracerebroventricular infusion of human A β 1-42 in Tg-SREBP-2 mice. Staining with an antibody that recognizes human A β (but not the endogenous mouse A β) demonstrated diffuse amyloid deposition in the hippocampus of A β -infused mice (for 28 days) (Fig. 5A). Quantitative determination by ELISA revealed equivalent A β loading in wild type mice and Tg-SREBP-2 mice (54.2 ± 14.6 and 66 ± 11.2 nmol/mg prot., respectively). Moreover, confocal analysis showed a significant co-localization of A β with cytochrome c staining (Fig. 5B), indicating that a fraction of the infused A β targeted mitochondria. Of note, endogenous brain A β 1-42 levels were similar in WT and Tg-SREBP-2 mice (Supplemental Fig. S7).

Neuroinflammation, manifested as activated microglia and astrocytes close to A β depositions, is an invariant characteristic of AD brain, which plays a key role in the progression of the disease by further amplifying A β generation and neuronal damage (Heneka and O'Banion, 2007). Greater microglia activation, determined by F4/80 immunostaining, was observed in the hippocampus of Tg-SREBP-2 mice infused with A β compared to vehicle-infused or A β -infused wild type mice (Fig. 5C). Astrocyte activation, manifested as GFAP immunoreactivity, was also elevated in hippocampal regions of A β -infused Tg-SREBP-2 mice (Fig. 5C). Moreover, confocal analysis of A β -infused Tg-SREBP-2 brains revealed the presence of microglia and astrocytes co-localizing with A β in amyloid deposits (Supplemental Fig. S8). These histological analyses were complemented by quantitative measurements of mRNA levels of pro-inflammatory cytokines such as TNF- α and IL-1 β . Increased expression of TNF-

α and IL-1 β was only observed in Tg-SREBP-2 brains infused with A β (Fig. 5D). Thus, Tg-SREBP-2 mice are more susceptible to A β -induced neuroinflammation.

Increased oxidative stress, synaptodendritic degeneration and neuronal damage in Tg-SREBP-2 mice following A β infusion

We next assessed the susceptibility of Tg-SREBP-2 mice to A β -induced oxidative stress and neurodegeneration. Malondialdehyde (MDA), an end product of lipid peroxidation, and accumulation of oxidized proteins assessed by carbonyl protein immunoblotting were significantly higher in the brain of A β -infused Tg-SREBP-2 mice compared to A β -infused wild type mice, with no signs of oxidative stress detected in brains of vehicle-infused wild type or Tg-SREBP-2 mice (Fig. 6A, B). Previous studies have shown that synaptic injury is an early event in the progression of AD, which correlates with the severity of cognitive deficits in AD patients (Masliah et al., 1994). As shown, the levels of the pre-synaptic protein synaptophysin were significantly lower in Tg-SREBP-2 mice infused with A β compared to wild type mice or vehicle-infused brains (Fig. 6C), indicating extensive synaptic loss. In addition, neuronal death and apoptosis estimated by Fluoro-Jade B-positive degenerating neurons and TUNEL staining, respectively, were higher in Tg-SREBP-2 mice following intracerebroventricular A β infusion compared to wild type mice (Fig. 6D, E). These data underscore the susceptibility of Tg-SREBP-2 mice to A β -induced neurodegeneration.

GSH ethyl ester co-infusion restores mGSH and protects against A β -induced neurodegeneration in Tg-SREBP-2 mice

To address whether the exacerbated inflammation and neuronal death of Tg-SREBP-2 mice following A β infusion is promoted by cholesterol-mediated mGSH depletion, GSH ethyl ester (GSHee), a membrane-permeable form of GSH, was co-infused with A β . GSHee significantly increased the mitochondrial pool of GSH in Tg-SREBP-2 mice (3.2 ± 0.2 vs. 1.4 ± 0.5 nmol/mg prot.), preventing A β -induced increase in MDA levels (Fig. 6F) and protein oxidation estimated by carbonyl protein immunoreactivity (Supplemental Fig. S9A). Moreover, reactive astrogliosis and microgliosis, determined by GFAP and F4/80 immunoreactivity, respectively, were also reduced in Tg-SREBP-2 mice when GSHee was co-infused with A β (Supplemental Fig. S9B). This outcome correlated with a significant decrease in the mRNA expression of the pro-inflammatory cytokines TNF- α and IL-1 β (Fig. 6G). In addition, neuronal damage, assessed by Fluoro-Jade B staining and TUNEL assay, in the hippocampal regions of A β -infused Tg-SREBP-2 brains was prevented by GSHee co-infusion (Fig. 6D, E). We further analyzed whether i.p. administration of GSHee was therapeutic against A β -induced neuroinflammation and neuronal loss. As seen, i.p. GSHee administration during the A β infusion period significantly increased mGSH content (Fig. 7A), attenuating MDA levels (Fig. 7B) and carbonyl protein immunoblotting (Fig. 7C), indicative of oxidative stress induced by A β in Tg-SREBP-2 mice. In addition, the enhanced presence of reactive astrocytes (Fig. 7D) and the upregulated expression of TNF- α (Fig. 7E) observed in A β -infused transgenic mice were significantly prevented by GSHee therapy, which correlates with a significant decrease in neuronal damage (Fig. 7F). Thus, these data indicate that strategies that boost mGSH such as GSHee protect against A β -induced neurodegeneration.

Enhanced mitochondrial cholesterol loading and mGSH depletion in APP/PS1 transgenic mice

In order to address the relevance of the preceding findings in AD, we examined the mitochondrial cholesterol and GSH content in a genetic mouse model of AD, namely, APP/PS1 transgenic mice. Brain mitochondria were isolated from 4-, 7-, and 10-months old APP/PS1 transgenic mice. As seen (Fig. 8A), mitochondrial cholesterol levels were unchanged in 4 and 7-months old transgenic mice, increasing twice as much in 10-months old APP/PS1

transgenic mice compared to wild type mice of the same age. As expected from our findings in Tg-SREBP-2 and NPC1^{-/-} mice, the mGSH levels decreased only in 10-months old APP/PS1 transgenic mice (Fig. 8B). Preceding the mitochondrial cholesterol loading and the subsequent mGSH depletion, we observed a significant generation of A β detected by ELISA in 4-months old APP/PS1 mice (not shown). Furthermore, either SREBP-2 mRNA and protein levels were significantly elevated in Tg-APP/PS1 mice (Fig. 8C, D), indicating that activation of SREBP-2 may contribute to the increase in cholesterol content. Thus, these findings lend further support for the relevance of enhanced mitochondrial cholesterol levels in AD.

Discussion

Epidemiological, genetic and biochemical studies have identified cholesterol, A β and mitochondria as key factors in AD pathogenesis, but the specific relationship of this triad has not been addressed before. In particular, the role of cholesterol in AD examined thus far has been limited to the amyloidogenic processing of APP at the plasma membrane to generate A β . In this regard, varying proportions of the presenilins and other components of the γ -secretase complex (nicastrin, Aph-1 and Pen-2), along with γ -secretase activity and the β -secretase BACE1, are present in detergent-resistant cholesterol-enriched lipid rafts (Taylor and Hooper, 2007). In addition, the activities of BACE1 and γ -secretase are stimulated by rafts lipid components, such as glycosphingolipids and cholesterol (Kalvodova et al., 2005; Osenkowski et al., 2008; Ariga et al., 2008). Intriguingly, although the presence of APP in detergent-resistant rafts is relatively minor (Lee et al., 1998), once localized to the raft, the APP may be rapidly cleaved by β - and γ -secretases, thus contributing to A β generation. Moreover, previous studies have shown that cholesteryl-ester levels directly correlate with A β production (Puglielli et al., 2001) and that statins inhibit the dimerization of β -secretase via both isoprenoid- and cholesterol-mediated mechanisms (Parsons et al., 2006).

In the current study, we examined the role of cholesterol in AD from an unusual perspective and provide evidence linking mitochondrial cholesterol to A β neurotoxicity, consistent with and expanding the recognized role of mitochondrial dysfunction in AD (Manzack et al., 2006; Caspersen et al., 2005; Lin and Beal, 2006; Lustbader et al., 2004; Casley et al., 2002). In addition to being targets of A β toxicity, it is conceivable that mitochondria may constitute an additional source of A β generation, in agreement with the presence of APP in mitochondria from AD-vulnerable brain regions (Devi et al., 2006), and the finding of functional complexes of APP with γ -secretase and IDE in mitochondria (Hansson et al., 2004; Leissring et al., 2004), arguing that these organelles may contribute to the amyloidogenic APP processing and hence A β generation. Regardless of the source of A β generation either via the more established pathway of APP processing at the plasma membrane, particularly in cholesterol-enriched domains, or its *in situ* generation in mitochondria, we provide evidence that mitochondrial cholesterol accumulation stands as a critical determinant of A β toxicity both *in vitro* and *in vivo* using Tg-SREBP-2 and NPC1^{-/-} mice.

It has been described that SREBP-2 downregulates the expression of genes which control brain A β clearance, such as LDLR-related protein 1 (also known as LRP) (Deane et al., 2004). Moreover, recent studies in AD patients and two mouse models of AD show that overexpression of serum response factor and myocardin in cerebral vascular smooth muscle cells (VSMC) generates an A β non-clearing VSMC phenotype through transactivation of SREBP-2, which is associated with A β accumulation (Bell et al., 2008); thus, it is conceivable that Tg-SREBP-2 may exhibit increased brain A β content secondary to lower LRP1 expression. Although we did not examine the expression level of LRP1, we did observe that the content of endogenous A β was similar in WT and Tg-SREBP-2 mice. These unexpected findings are consistent with evidence indicating that LRP1 promotes APP endocytosis and its processing to A β production (Ulery et al. 2000; Zerbinatti et al., 2004).

In agreement with the downregulation of mGSH by increased cholesterol-mediated impairment of mGSH transport from cytosol (Mari et al., 2006; Colell et al., 1997; Mari et al., 2008), we observed that isolated mitochondria from both Tg-SREBP-2 mice and NPC1 knockout mice exhibit mGSH depletion and enhanced susceptibility to A β -mediated toxicity and mitochondrial membrane permeabilization. Although GSH exists in both cytosol and mitochondria, this latter pool has been shown to control the susceptibility to stimuli that trigger mitochondrial oxidative stress including TNF, Fas or hypoxia (Mari et al., 2006; Colell et al., 1997; Mari et al., 2008; Lluís et al., 2006). However, although total GSH depletion and altered GSH redox cycle has been described in AD, the particular pool of mGSH in modulating A β toxicity has not been specifically addressed. Two lines of evidence indicate that the mGSH depletion specifically accounted for the increased susceptibility to A β observed in these genetic models. First, the sensitivity of rat brain mitochondria to A β -mediated oxidative stress and release of intermembrane apoptotic proteins was dependent on the levels of mGSH. Second, selective pharmacological depletion of mGSH with the spare of cytosol GSH in human neuroblastoma and glial cells sensitized to A β -mediated cell death. Hence these findings expand the role of cholesterol in A β neurotoxicity, indicating that in addition to fostering the amyloidogenic processing of APP, mitochondrial cholesterol modulates A β neurotoxicity via mGSH regulation. Interestingly, recent findings have shown that hydrogen peroxide promotes A β production through JNK-dependent activation of γ -secretase (Shen et al., 2008), implying that in addition to the modulation of A β toxicity, enhanced mitochondrial cholesterol-mediated mGSH depletion may activate an autoamplification loop by stimulating oxidative stress to further generate A β , thus establishing a toxic vicious cycle.

Although increased cholesterol levels have been described in membranes from brain tissue samples of AD patients (Bandaru et al., 2007; Cutler et al., 2004), the specific pool of mitochondrial cholesterol has not been previously reported to the best of our knowledge. However, enhanced immunocytochemical localization of steroidal acute regulatory protein (StAR) has been described in the pyramidal hippocampal neurons of AD-affected patients (Webber et al., 2006). Given the role of StAR in the mitochondrial transport of cholesterol (Soccio and Breslow, 2004) and hence in the modulation of mitochondrial cholesterol levels (Montero et al., 2008), the increased expression of StAR in AD patients, would strongly suggest that mitochondrial cholesterol accumulation may actually occur in patients with AD. Indeed, in the current study, we observed mitochondrial cholesterol loading and subsequent mGSH depletion in APP/PS1 transgenic mice, a genetic mouse model of AD, and interestingly, these changes in mitochondria were preceded by A β accumulation in the brain of APP/PS1 mice. Based on this temporal relationship, it is tempting to speculate that A β may regulate cholesterol homeostasis and/or trafficking. Although this needs to be specifically addressed, consistent with this possibility, previous studies underscored that A β 1-40/1-42 ratio altered lipid homeostasis and that familial presenilin mutations decreased the A β 1-40/1-42 ratio resulting in enhanced cholesterol levels (Grimm et al., 2005), suggesting that A β generation contributed to increased cholesterol content. A complication in this possible scenario of mutual regulation between cholesterol and A β is the observation that cholesteryl-esters unlike free cholesterol modulated A β generation (Puglielli et al., 2001).

Previous studies described the requirement for functional mitochondria in A β -mediated neurotoxicity and that A β interacts with the regulatory heme of complex IV leading to mitochondrial dysfunction and ROS production (Cardoso et al., 2001; Atamna and Boyle, 2006). Through inhibition of electron flow at different mitochondrial respiratory complexes, we show that complex III is a major site for mitochondrial ROS by A β , whose levels increased if mGSH levels are low, resulting in mitochondrial depolarization, release of cytochrome c, and caspase-3 activation. Interestingly caspase inhibition failed to protect mGSH-dependent sensitization of SH-SY5Y cells to A β -mediated cell death despite efficiently preventing the acquisition of apoptotic features, suggesting that A β stimulated both an oxidant-dependent cell

death pathway and caspase-independent apoptosis pathways, which are modulated by mGSH levels.

Our *in vivo* studies underscore a higher sensitivity of Tg-SREBP-2 mice to infusion of human A β , resulting in enhanced lipid peroxidation, oxidative modification of proteins, glia activation, indicative of neuroinflammation, and neuronal damage. Although cholesterol upregulation in Tg-SREBP-2 did not modulate endogenous A β generation, we observed that a significant fraction of infused human A β co-localized with mitochondria, pointing to the mitochondria as a target of the A β toxicity *in vivo*. To substantiate that the increased susceptibility of Tg-SREBP-2 mice to *in vivo* A β infusion was mediated by mitochondrial cholesterol-induced mGSH depletion, we tested the role of co-infusing A β with GSH ethyl ester. GSH ethyl ester is a membrane permeable form of GSH, which unlike GSH precursors such as N-acetylcysteine increases mGSH independently of the transport of GSH into mitochondria (Mari et al., 2006; Mari et al., 2008). This implies that GSH ethyl ester bypasses the block of cytosol GSH transport into mitochondria imposed by cholesterol-mediated membrane dynamics, thus leading to mGSH replenishment (Mari et al., 2006; Colell et al., 1997; Mari et al., 2008). The downregulation of oxidative stress, neuroinflammation and protection against *in vivo* infusion of A β in Tg-SREBP-2 via mGSH recovery highlights the relevance of mitochondrial cholesterol-mediated regulation of mGSH in A β -induced neurodegeneration. From a therapeutic perspective, the fact that the particular pool of mGSH rather than cytosol GSH determines A β susceptibility implies that efforts should focus to specifically replenish mGSH to slow down disease progression. The therapeutic usefulness of this strategy is illustrated here by the ability of i.p. administration of GSH ethyl ester in protecting against A β -induced neuroinflammation and neuronal loss. In addition to directly modulating mGSH by GSH ethyl ester, targeting the increased pool of mitochondrial cholesterol may be of relevance in AD, as it would be expected to restore mGSH levels. In line with this possibility, it was shown in obese ob/ob mice that atorvastatin therapy was useful in preventing susceptibility to TNF-mediated steatohepatitis by preventing mitochondrial cholesterol loading which subsequently resulted in increased mGSH levels (Mari et al., 2006). Taking this precedent as well as the previous suggestions for the use of statins in AD (Wolozin et al., 2000; Fassbender et al., 2001; Parsons et al., 2006), the therapeutic combination of statins plus GSH ethyl ester may be of potential therapeutic significance in AD.

Supplementary Material

Refer to Web version on PubMed Central for supplementary material.

Acknowledgments

This work was supported in part by the Plan Nacional de I+D Grants: SAF2005-03923 and SAF2006-06780, by the Research Center for Liver and Pancreatic Diseases Grant P50 AA 11999 funded by the US National Institute on Alcohol Abuse and Alcoholism, and by the Centro de Investigacion Biomedica en Red de Enfermedades Hepaticas y Digestivas (CIBEREHD) supported by the Instituto de Salud Carlos III. We are grateful to Dr. M. Guzman from Complutense University, Madrid, for kindly providing the glia derived cell lines. The technical assistance of Alberto García-Martínez is highly appreciated. We thank the Servicio Científico-técnico of IDIBAPS for EM, confocal imaging, and flow cytometry analysis assistance and Dr. C. Sanmartin from Navarra University, for the HP synthesis. We thank Drs. C. Garcia-Ruiz, M. Mari and A. Morales for critical reading the manuscript. A.C. is supported by the Ramon y Cajal Research Program (MEC). This work is dedicated to patients suffering Alzheimer's disease, in particular Faustina Torres Muñoz who recently passed away as a victim of this devastating disease.

References

Anstey KJ, Lipnicki DM, Low LF. Cholesterol as a risk factor for dementia and cognitive decline: a systematic review of prospective studies with meta-analysis. *Am J Geriatr Psychiatry* 2008;16:343–354. [PubMed: 18448847]

- Ariga T, McDonald MP, Yu RK. Role of ganglioside metabolism in the pathogenesis of Alzheimer's disease--a review. *J Lipid Res* 2008;49:1157–1175. [PubMed: 18334715]
- Atamna H, Boyle K. Amyloid-beta peptide binds with heme to form a peroxidase: relationship to the cytopathologies of Alzheimer's disease. *Proc Natl Acad Sci USA* 2006;103:3381–3386. [PubMed: 16492752]
- Bandaru VV, Troncoso J, Wheeler D, Pletnikova O, Wang J, Conant K, Haughey NJ. ApoE4 disrupts sterol and sphingolipid metabolism in Alzheimer's but not normal brain. *Neurobiol Aging*. 2007;10.1016/j.neurobiolaging.2007.07.024
- Bell RD, Deane R, Chow N, Long X, Sagare A, Singh I, Streb JW, Guo H, Rubio A, Van Nostrand W, Miano JM, Zlokovic BV. SRF and myocardin regulate LRP-mediated amyloid-beta clearance in brain vascular cells. *Nat Cell Biol* 2009;11:143–153. [PubMed: 19098903]
- Boyd-Kimball D, Sultana R, Abdul HM, Butterfield DA. Gamma-glutamylcysteine ethyl ester-induced up-regulation of glutathione protects neurons against Abeta(1-42)-mediated oxidative stress and neurotoxicity: implications for Alzheimer's disease. *J Neurosci Res* 2005;79:700–706. [PubMed: 15678514]
- Cardoso SM, Santos S, Swerdlow RH, Oliveira CR. Functional mitochondria are required for amyloid beta-mediated neurotoxicity. *FASEB J* 2001;15:1439–1441. [PubMed: 11387250]
- Casley CS, Canevari L, Land JM, Clark JB, Sharpe MA. Beta-amyloid inhibits integrated mitochondrial respiration and key enzyme activities. *J Neurochem* 2002;80:91–100. [PubMed: 11796747]
- Caspersen C, Wang N, Yao J, Sosunov A, Chen X, Lustbader JW, Xu HW, Stern D, McKhann G, Yan SD. Mitochondrial Abeta: a potential focal point for neuronal metabolic dysfunction in Alzheimer's disease. *FASEB J* 2005;19:2040–2041. [PubMed: 16210396]
- Colell A, García-Ruiz C, Morales A, Ballesta A, Ookhtens M, Rodés J, Kaplowitz N, Fernández-Checa JC. Transport of reduced glutathione in hepatic mitochondria and mitoplasts from ethanol-treated rats: effect of membrane physical properties and S-adenosyl-L-methionine. *Hepatology* 1997;26:699–708. [PubMed: 9303501]
- Cutler RG, Kelly J, Storie K, Pedersen WA, Tammara A, Hatanpaa K, Troncoso JC, Mattson MP. Involvement of oxidative stress-induced abnormalities in ceramide and cholesterol metabolism in brain aging and Alzheimer's disease. *Proc Natl Acad Sci USA* 2004;101:2070–2075. [PubMed: 14970312]
- Deane R, Wu Z, Sagare A, Davis J, Du Yan S, Hamm K, Xu F, Parisi M, LaRue B, Hu HW, Spijkers P, Guo H, Song X, Lenting PJ, Van Nostrand WE, Zlokovic BV. LRP/amyloid beta-peptide interaction mediates differential brain efflux of Abeta isoforms. *Neuron* 2004;43:333–344. [PubMed: 15294142]
- Deane R, Zlokovic BV. Role of blood brain barrier in the pathogenesis of Alzheimer's disease. *Curr Alzheimer Res* 2007;4:191–197. [PubMed: 17430246]
- Devi L, Prabhu BM, Galat DF, Avadhani NG, Anandatheerthavarada HK. Accumulation of amyloid precursor protein in the mitochondrial import channels of human Alzheimer's disease brain is associated with mitochondrial dysfunction. *J Neurosci* 2006;26:9057–9068. [PubMed: 16943564]
- Fassbender K, Simons M, Bergmann C, Stroick M, Lutjohann D, Keller P, Runz H, Kuhl S, Bertsch T, von Bergmann K, Hennerici M, Beyreuther K, Hartmann T. Simvastatin strongly reduces levels of Alzheimer's disease β -amyloid peptides A β 42 and A β 40 in vitro and in vivo. *Proc Natl Acad Sci USA* 2001;98:5856–5861. [PubMed: 11296263]
- Fernandez-Checa JC, Ookhtens M, Kaplowitz N. Effect of chronic ethanol feeding on rat hepatocytic glutathione: compartmentation, efflux and response to incubation with ethanol. *J Clin Invest* 1987;80:57–62. [PubMed: 2885343]
- Fernandez-Checa JC, Kaplowitz N. Hepatic mitochondrial glutathione: transport and role in disease and toxicity. *Toxicol Appl Pharmacol* 2005;204(3):263–273. [PubMed: 15845418]
- Frantschy SA, Yang F, Calderon L, Cole GM. Rodent models of Alzheimer's disease: rat A β infusion approaches to amyloid deposits. *Neurobiol Aging* 1996;17:311–321. [PubMed: 8744413]
- García-Ruiz C, Colell A, Marí M, Morales A, Calvo M, Enrich C, Fernández-Checa JC. Defective TNF- α -mediated hepatocellular apoptosis and liver damage in acidic sphingomyelinase knockout mice. *J Clin Invest* 2003;111:197–208. [PubMed: 12531875]

- Grimm MO, Grimm HS, Pätzold AJ, Zinser EG, Halonen R, Duering M, Tschäpe JA, De Strooper B, Müller U, Shen J, Hartmann T. Regulation of cholesterol and sphingomyelin metabolism by amyloid beta and presenilin. *Nat Cell Biol* 2005;7:1118–1123. [PubMed: 16227967]
- Haass C, Selkoe DJ. Soluble protein oligomers in neurodegeneration: lessons from the Alzheimer's amyloid beta-peptide. *Nat Rev Mol Cell Biol* 2007;8:101–112. [PubMed: 17245412]
- Hansson CA, Frykman S, Farmery MR, Tjernberg LO, Nilsberth C, Pursglove SE, Ito A, Winblad B, Cowburn RF, Thyberg J, Ankarcrona M. Nicastrin, presenilin, APH-1, and PEN-2 form active gamma-secretase complexes in mitochondria. *J Biol Chem* 2004;279:51654–51660. [PubMed: 15456764]
- Heneka MT, O'Banion MK. Inflammatory processes in Alzheimer's disease. *J Neuroimmunol* 2007;184:69–91. [PubMed: 17222916]
- Horton JD, Shimomura I, Brown MS, Hammer RE, Goldstein JL, Shimano H. Activation of cholesterol synthesis in preference to fatty acid synthesis in liver and adipose tissue of transgenic mice overproducing sterol regulatory element-binding protein-2. *J Clin Invest* 1998;101:2331–2339. [PubMed: 9616204]
- Horton JD, Goldstein JL, Brown MS. SREBPs: activators of the complete program of cholesterol and fatty acid synthesis in the liver. *J Clin Invest* 2002;109:1125–1131. [PubMed: 11994399]
- Hsiao K, Chapman P, Nilsen S, Eckman C, Harigaya Y, Younkin S, Yang F, Cole G. Correlative memory deficits, A β elevation, and amyloid plaques in transgenic mice. *Science* 1996;274:99–102. [PubMed: 8810256]
- Jain A, Mårtensson J, Stole E, Auld PA, Meister A. Glutathione deficiency leads to mitochondrial damage in brain. *Proc Natl Acad Sci USA* 1991;88:1913–1917. [PubMed: 2000395]
- Kalvodova L, Kahya N, Schwille P, Eehalt R, Verkade P, Drechsel D, Simons K. Lipids as modulators of proteolytic activity of BACE: involvement of cholesterol, glycosphingolipids, and anionic phospholipids in vitro. *J Biol Chem* 2005;280:36815–36823. [PubMed: 16115865]
- Lee SJ, Liyanage U, Bickel PE, Xia W, Lansbury PT Jr, Kosik KS. A detergent-insoluble membrane compartment contains A β in vivo. *Nat Med* 1998;4:730–734. [PubMed: 9623986]
- Leissring MA, Farris W, Wu X, Christodoulou DC, Haigis MC, Guarente L, Selkoe DJ. Alternative translation initiation generates a novel isoform of insulin-degrading enzyme targeted to mitochondria. *Biochem J* 2004;383:439–446. [PubMed: 15285718]
- Lin MT, Beal MF. Mitochondrial dysfunction and oxidative stress in neurodegenerative diseases. *Nature* 2006;443:787–795. [PubMed: 17051205]
- Lluis JM, Buricchi F, Chiarugi P, Morales A, Fernandez-Checa JC. Dual role of mitochondrial reactive oxygen species in hypoxia signaling: activation of nuclear factor- κ B via c-SRC and oxidant-dependent cell death. *Cancer Res* 2006;67:7368–7377. [PubMed: 17671207]
- Lustbader JW, et al. ABAD directly links A β to mitochondrial toxicity in Alzheimer's disease. *Science* 2004;304:448–452. [PubMed: 15087549]
- Manczak M, Anekonda TS, Henson E, Park BS, Quinn J, Reddy PH. Mitochondria are a direct site of A β accumulation in Alzheimer's disease neurons: implications for free radical generation and oxidative damage in disease progression. *Hum Mol Genet* 2006;15:1437–1449. [PubMed: 16551656]
- Marí M, Caballero F, Colell A, Morales A, Caballeria J, Fernandez A, Enrich C, Fernandez-Checa JC, García-Ruiz C. Mitochondrial free cholesterol loading sensitizes to TNF- and Fas-mediated steatohepatitis. *Cell Metab* 2006;4:185–198. [PubMed: 16950136]
- Marí M, Colell A, Morales A, Caballero F, Moles A, Fernández A, Terrones O, Basañez G, Antonsson B, García-Ruiz C, Fernández-Checa JC. Mechanism of mitochondrial glutathione-dependent hepatocellular susceptibility to TNF despite NF- κ B activation. *Gastroenterology* 2008;134:1507–1520. [PubMed: 18343380]
- Martensson J, Han J, Griffith OW, Meister A. Glutathione ester delays the onset of scurvy in ascorbate-deficient guinea pigs. *Proc Natl Acad Sci U S A* 1993;90:317–321. [PubMed: 8419936]
- Masliah E, Mallory M, Hansen L, DeTeresa R, Alford M, Terry R. Synaptic and neuritic alterations during the progression of Alzheimer's disease. *Neurosci Lett* 1994;174:67–72. [PubMed: 7970158]
- Mattson MP. Pathways towards and away from Alzheimer's Disease. *Nature* 2004;430:631–639. [PubMed: 15295589]

- Montero J, Morales A, Llacuna L, Lluís JM, Terrones O, Basañez G, Antonsson B, Prieto J, García-Ruiz C, Colell A, Fernández-Checa JC. Mitochondrial cholesterol contributes to chemotherapy resistance in hepatocellular carcinoma. *Cancer Res* 2008;68:5246–5256. [PubMed: 18593925]
- Norman AW, Demel RA, de Kruffyff B, van Deenen LL. Studies on the biological properties of polyene antibiotics. Evidence for the direct interaction of filipin with cholesterol. *J Biol Chem* 1972;247:1918–1929. [PubMed: 5012767]
- Notkola IL, Sulkava R, Pekkanen J, Erkinjuntti T, Ehnholm C, Kivinen P, Tuomilehto J, Nissinen A. Serum total cholesterol, apolipoprotein E 4 allele, and Alzheimer's disease. *Neuroepidemiology* 1998;17:14–20. [PubMed: 9549720]
- Oddo S, Caccamo A, Shepherd JD, Murphy MP, Golde TE, Kaye R, Metherate R, Mattson MP, Akbari Y, LaFerla FM. Triple-transgenic model of Alzheimer's disease with plaques and tangles: intracellular Abeta and synaptic dysfunction. *Neuron* 2003;39:409–421. [PubMed: 12895417]
- Osenkowski P, Ye W, Wang R, Wolfe MS, Selkoe DJ. Direct and potent regulation of gamma-secretase by its lipid microenvironment. *J Biol Chem* 2008;283:22529–22540. [PubMed: 18539594]
- Paul CA, Boegle AK, Maue RA. Before the loss: neuronal dysfunction in Niemann-Pick Type C disease. *Biochim Biophys Acta* 2004;1685:63–76. [PubMed: 15465427]
- Parsons RB, Price C, Farrant JK, Subramaniam D, Adeagbo-sheikh J, Austen BM. Statins inhibit the dimerization of b-secretase via both isoprenoid and cholesterol-mediated mechanisms. *Biochem J* 2006;399:205–214. [PubMed: 16803455]
- Pirttilä T, Soininen H, Mehta PD, Heinonen O, Lehtimäki T, Bogdanovic N, Paljärvi L, Kim KS, Kosunen O, Winblad B, Riekkinen P Sr, Wisniewski HM. Apolipoprotein E genotype and amyloid load in Alzheimer disease and control brains. *Neurobiol Aging* 1997;18:121–127. [PubMed: 8983040]
- Puglielli L, Konopka G, Pack-Chung E, MacKenzie Ingano LA, Berezovska O, Hyman BT, Chang TY, Tanzi RE, Kovacs DM. Acyl-coenzyme A:cholesterol acyltransferase modulates the generation of the amyloid b-peptide. *Nat Cell Biol* 2001;3:905–912. [PubMed: 11584272]
- Resende R, Moreira PI, Proença T, Deshpande A, Busciglio J, Pereira C, Oliveira CR. Brain oxidative stress in a triple-transgenic mouse model of Alzheimer disease. *Free Radic Biol Med* 2008;44:2051–2057. [PubMed: 18423383]
- Schönknecht P, Lütjohann D, Pantel J, Bardenheuer H, Hartmann T, von Bergmann K, Beyreuther K, Schröder J. Cerebrospinal fluid 24S-hydroxycholesterol is increased in patients with Alzheimer's disease compared to healthy controls. *Neurosci Lett* 2002;324:83–85. [PubMed: 11983301]
- Selkoe DJ. Developing preventive therapies for chronic diseases: lessons learned from Alzheimer's disease. *Nutr Rev* 2007;65:S239–243. [PubMed: 18240556]
- Shankar GM, Li S, Mehta TH, Garcia-Munoz A, Shepardson NE, Smith I, Brett FM, Farrell MA, Rowan MJ, Lemere CA, Regan CM, Walsh DM, Sabatini BL, Selkoe DJ. Amyloid-beta protein dimers isolated directly from Alzheimer's brains impair synaptic plasticity and memory. *Nat Med* 2008;14:837–842. [PubMed: 18568035]
- Shen C, Chen Y, Liu H, Zhang K, Zhang T, Lin A, Jing N. Hydrogen peroxide promotes A β production through JNK-dependent activation of g-secretase. *J Biol Chem* 2008;283:17721–17730. [PubMed: 18436531]
- Soccio RE, Breslow JL. Intracellular cholesterol transport. *Arterioscler Thromb Vas Biol* 2004;24:1150–1160.
- Tanzi RE, Moir RD, Wagne SL. Clearance of Alzheimer's Ab peptide: The many roads to perdition. *Neuron* 2004;43:605–608. [PubMed: 15339642]
- Taylor DR, Hooper NM. Role of lipid rafts in the processing of the pathogenic prion and Alzheimer's amyloid-beta proteins. *Semin Cell Dev Biol* 2007;18:638–644. [PubMed: 17822928]
- Tietze F. Enzymatic method for quantitative determination of nano-gram amounts of total and oxidized glutathione: application to mammalian blood and other tissues. *Anal Biochem* 1969;77:502–524. [PubMed: 4388022]
- Ulery PG, Beers J, Mikhailenko I, Tanzi RE, Rebeck GW, Hyman BT, Strickland DK. Modulation of beta-amyloid precursor protein processing by the low density lipoprotein receptor-related protein (LRP). Evidence that LRP contributes to the pathogenesis of Alzheimer's disease. *J Biol Chem* 2000;275:7410–7415. [PubMed: 10702315]

- Walsh DM, Selkoe DJ. Deciphering the molecular basis of memory failure in Alzheimer's Disease. *Neuron* 2004;44:181–193. [PubMed: 15450169]
- Webber KM, Stocco DM, Casadesus G, Bowen RL, Atwood CS, Preville LA, Harris PL, Zhu X, Perry G, Smith MA. Steroidogenic acute regulatory protein (StAR): evidence of gonadotropin-induced steroidogenesis in Alzheimer disease. *Mol Neurodegener* 2006;1:14. [PubMed: 17018137]
- Wolozin B, Kellman W, Ruosseau P, Celesia GG, Siegel G. Decreased prevalence of Alzheimer disease associated with 3-hydroxy-3-methylglutaryl coenzyme A reductase inhibitors. *Arch Neurol* 2000;57:1439–1443. [PubMed: 11030795]
- Yu W, Gong JS, Ko M, Garver WS, Yanagisawa K, Michikawa M. Altered cholesterol metabolism in Niemann-Pick type C1 mouse brains affects mitochondrial function. *J Biol Chem* 2005;280:11731–11739. [PubMed: 15644330]
- Zeevalk GD, Manzano L, Sonsalla PK, Bernard LP. Characterization of intracellular elevation of glutathione (GSH) with glutathione monoethyl ester and GSH in brain and neuronal cultures: relevance to Parkinson's disease. *Exp Neurol* 2007;203:512–520. [PubMed: 17049515]
- Zerbinatti CV, Wozniak DF, Cirrito J, Cam JA, Osaka H, Bales KR, Zhuo M, Paul SM, Holtzman DM, Bu G. Increased soluble amyloid-beta peptide and memory deficits in amyloid model mice overexpressing the low-density lipoprotein receptor-related protein. *Proc Natl Acad Sci U S A* 2004;101:1075–1080. [PubMed: 14732699]
- Zlokovic BV. Neurovascular mechanisms of Alzheimer's neurodegeneration. *Trends Neurosci* 2005;28:202–208. [PubMed: 15808355]

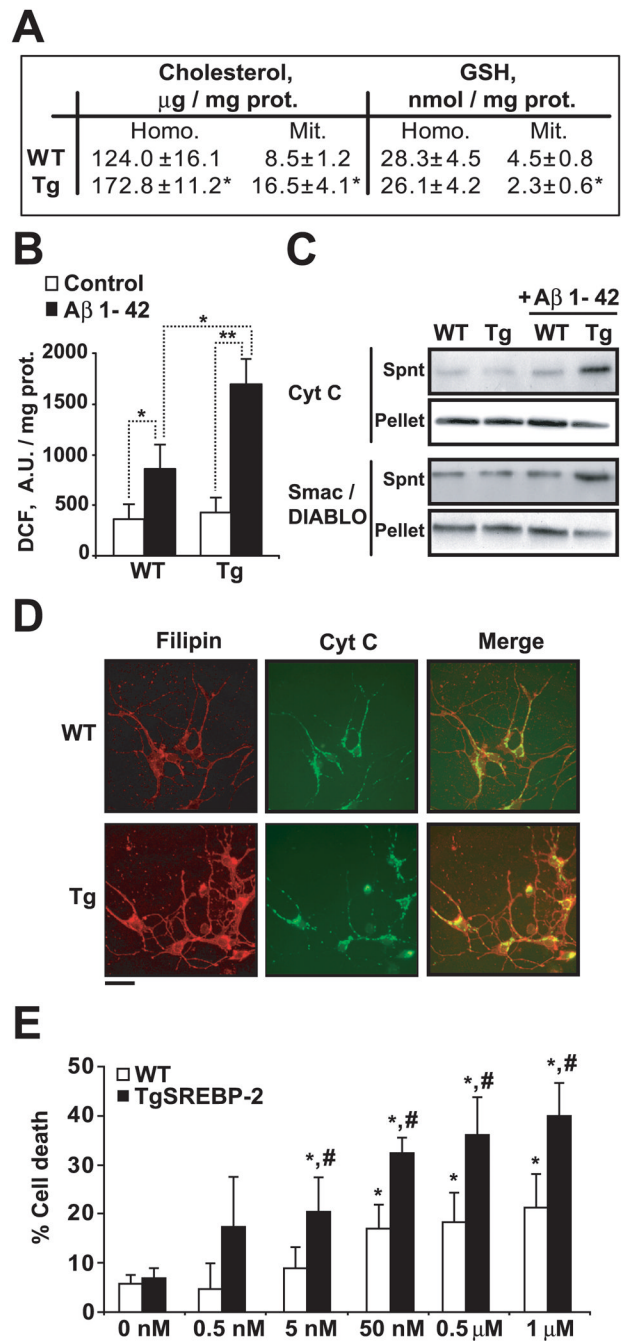


Figure 1. Increased susceptibility to A β 1-42 exposure of brain mitochondria and cortical neurons from SREBP-2 transgenic mice. **A**, Total cholesterol levels and GSH levels of brain homogenate (Homo.) and isolated mitochondria (Mit.) from wild type (WT) and SREBP-2 transgenic mice (Tg); * P <0.05 (n = 6–8 per genotype). **B** and **C**, Wild type (WT) and transgenic (TgSREBP-2) mitochondria (1 mg/ml) were exposed to A β 1-42 (1 μ M) for 2 h. **B**, Hydrogen peroxide generation determined by DCF fluorescence (A.U.: arbitrary units). * P <0.05, ** P <0.01 (n = 6–8 per genotype). **C**, After A β treatment mitochondria were pelleted and the resulting supernatants (spnt) and pellets were analyzed for the presence of apoptogenic proteins. Shown are representative immunoblottings of cytochrome c (Cyt C) and Smac/DIABLO (n = 4). **D**

and *E*, Primary neurons isolated from wild type (WT) and transgenic (TgSREBP-2) cerebral cortices at 6 DIV. *D*, Representative confocal images of cortical neurons stained with filipin (red) and mouse anti-cytochrome c antibody followed by the appropriated FITC-conjugated secondary antibody (Cyt C, green). Scale bars: 10 μm . *E*, Cell death of cortical neurons after exposure to increasing doses of A β 1-42 as indicated for 48 h. * $P < 0.05$ vs. untreated cells (0 nM), # $P < 0.01$ vs. WT cells ($n = 4-6$). Values are mean \pm S.D.; mean differences were compared by unpaired Student's t test.

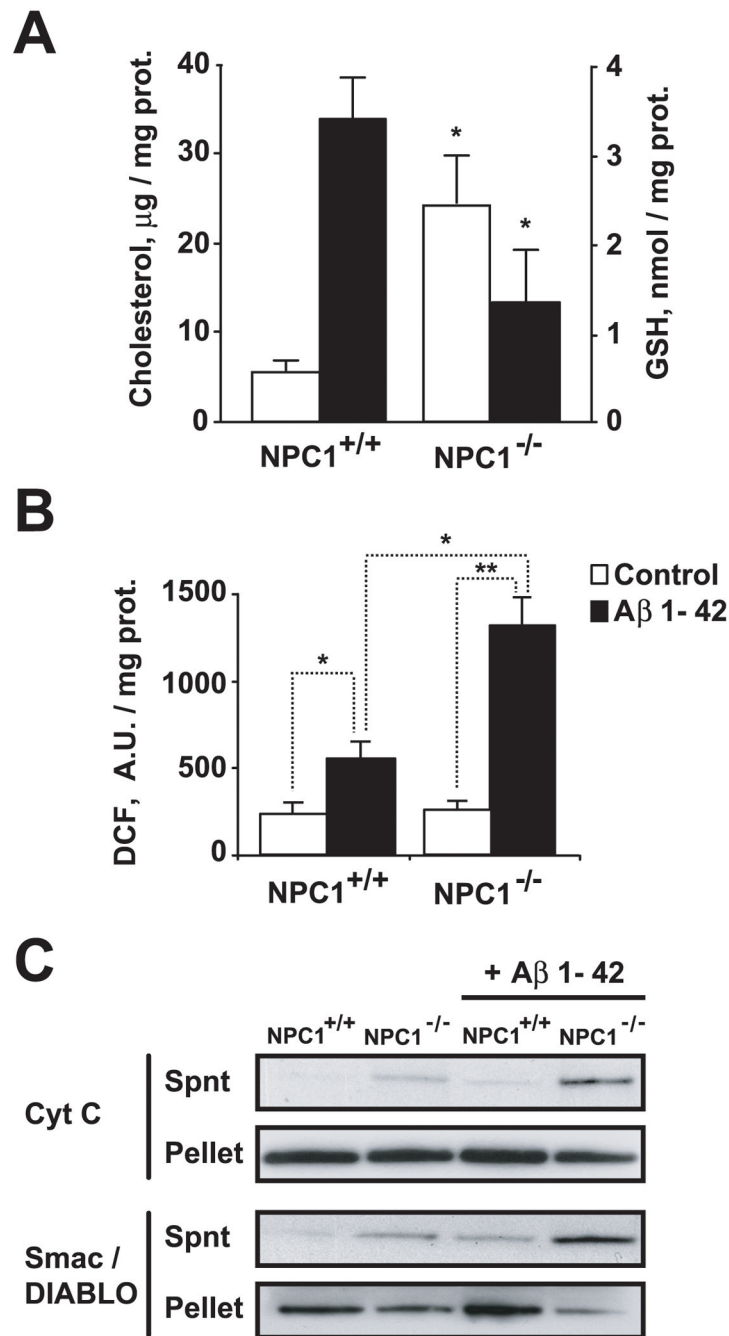
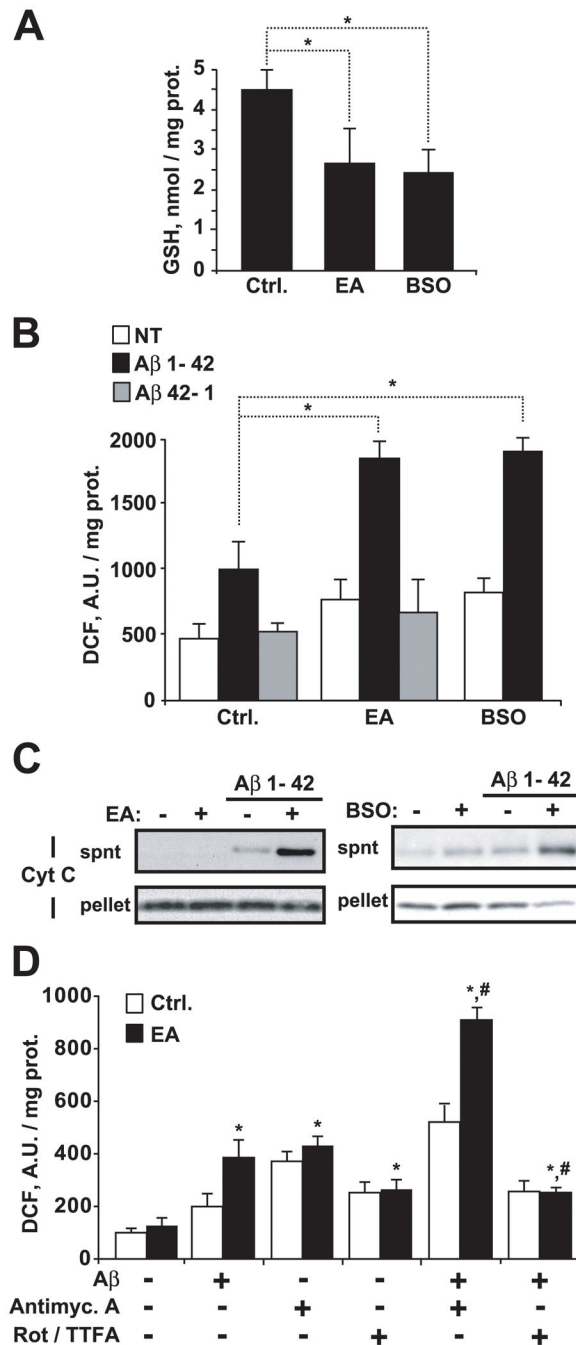


Figure 2. Isolated brain mitochondria from NPC1 knock-out mice show an increased sensitivity to A β 1-42. **A**, Total cholesterol levels (white bars) and GSH levels (black bars) of isolated mitochondria from NPC1^{+/+} and NPC1^{-/-} brains. * $P < 0.05$ ($n = 3-4$ per genotype). **B**, Hydrogen peroxide generation determined by DCF fluorescence of mitochondria (1mg/ml) incubated with A β 1-42 (1 μM) for 2 h. * $P < 0.05$, ** $P < 0.01$ ($n = 3-4$ per genotype). **C**, After 2 h treatment with A β 1-42 (1 μM) mitochondria were pelleted and the resulting supernatants (spnt) and pellets were analyzed by western blotting for the presence of cytochrome c (Cyt C) and Smac/DIABLO. Representative immunoblottings are shown. Values are mean \pm S.D.; mean differences were compared by unpaired Student's t test.

**Figure 3.**

Mitochondrial GSH regulates A β -induced oxidative stress. Depletion of mitochondrial GSH levels was assessed *in vitro* by incubation of isolated mitochondria (1 mg/ml) with 5 μ M ethacrynic acid (EA) for 15 min or *in vivo* by inhibiting the GSH synthesis with buthionine sulfoximine treatment (BSO, 3 mmol / kg). **A**, GSH levels following EA or BSO treatment. * $P < 0.05$ ($n = 4-6$). **B** and **C**, Mitochondria from rat brain pretreated with EA or BSO were exposed to A β 1-42 (5 μ M) or the inactive form A β 42-1 (5 μ M) for 2h. **B**, Hydrogen peroxide generation determined by DCF fluorescence (A.U.: arbitrary units; NT: untreated mitochondria). * $P < 0.05$ ($n = 4-6$). **C**, After A β treatment mitochondria were pelleted and the resulting supernatants (spnt) and pellets were analyzed for the presence of cytochrome c (Cyt

C) and Smac/DIABLO. Shown are representative immunoblottings of 3 independent experiments. **D**, Effect of blocking the electron transport chain at complex I, II, or III on the generation of hydrogen peroxide by A β . After EA treatment mitochondria were incubated with rotenone and TTFA (Rot/TTFA, 20 and 15 μ M, respectively), antimycin A (5 μ M), and / or A β (5 μ M) during 60 min. The blockers of the respiratory complexes were added 15 min before exposure to A β . Hydrogen peroxide generation was assessed by DCF fluorescence (A.U.: arbitrary units). * P <0.05 vs. untreated mitochondria; # P <0.01 vs. A β -treated mitochondria. (n = 3). Values are mean \pm S.D.; mean differences were compared by Dunnett's test.

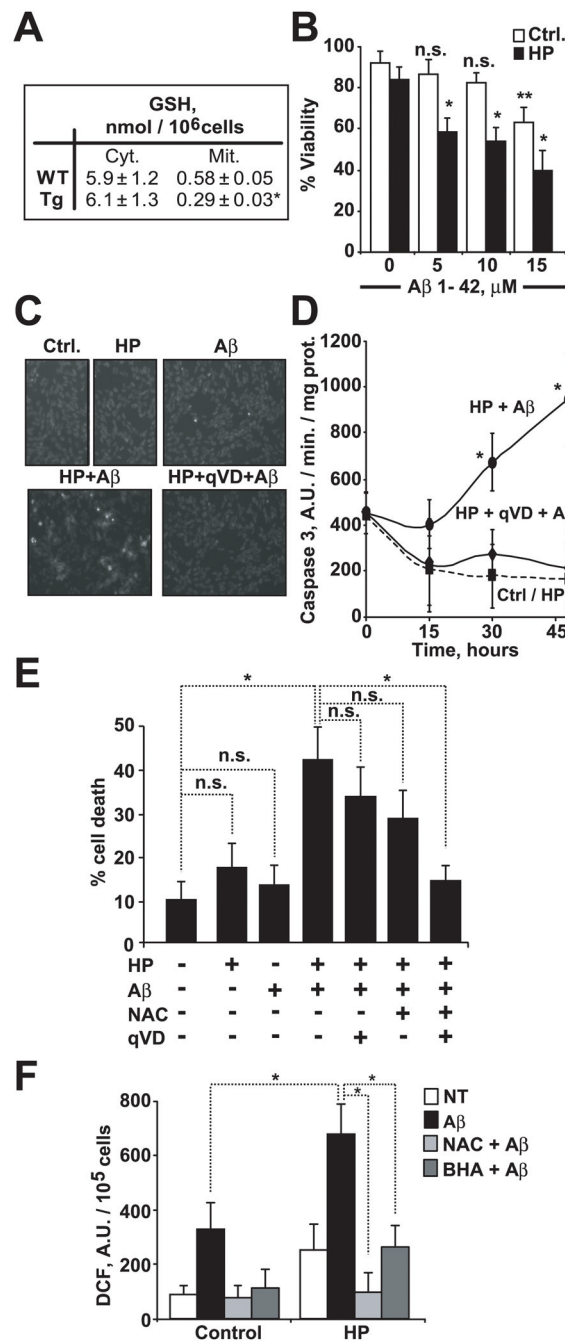


Figure 4. Selective depletion of mitochondrial GSH in human neuroblastoma SH-SY5Y cells enhances the apoptotic cell death induced by Aβ. Mitochondrial GSH depletion was assessed by incubating cells with (S)-3-hydroxy-4-pentenoate (HP, 5 mM) for 10 min. **A**, GSH levels. **P* = 0.002 (*n* = 4). **B**, Cell viability after 24 h incubation with increasing concentrations of Aβ1-42. **P* < 0.01 vs. HP-treated cells at 0 μM, ***P* = 0.02 vs. control cells at 0 μM, n.s.: not significant (*n* = 4). **C**, Chromatin morphology of cells exposed to Aβ1-42 (5 μM, 24 h) analyzed by Hoescht-33258 staining. Original magnification, 200×. (*n* = 4). **D**, Caspase-3 activity of cell extracts from cells exposed to Aβ1-42 (5 μM, 24 h) with or without the pancaspase inhibitor qVD-OPH (20 μM). **P* < 0.05 vs. HP-treated cells. (*n* = 3). **E** and **F**, After preincubation with

the antioxidants agents N-acetyl-cysteine (NAC, 3 mM) or butylated hydroxyanisole (BHA, 20 μ M) and / or the caspase inhibitor qVD-OPH (20 μ M) for 2 h, mitochondrial GSH was depleted by HP treatment and cells were exposed to A β 1-42 (5 μ M). ($n = 3-4$). **E**, Cell death analyzed by PI staining at 24 h exposure to A β 1-42. * $P < 0.01$, n.s.: not significant. **F**, Hydrogen peroxide generation after 2 h incubation with A β 1-42. * $P < 0.05$ (A.U.: arbitrary units). Values are mean \pm S.D.; mean differences were compared by Dunnett's test (**B**, **E** and **F**) or unpaired Student's t test.

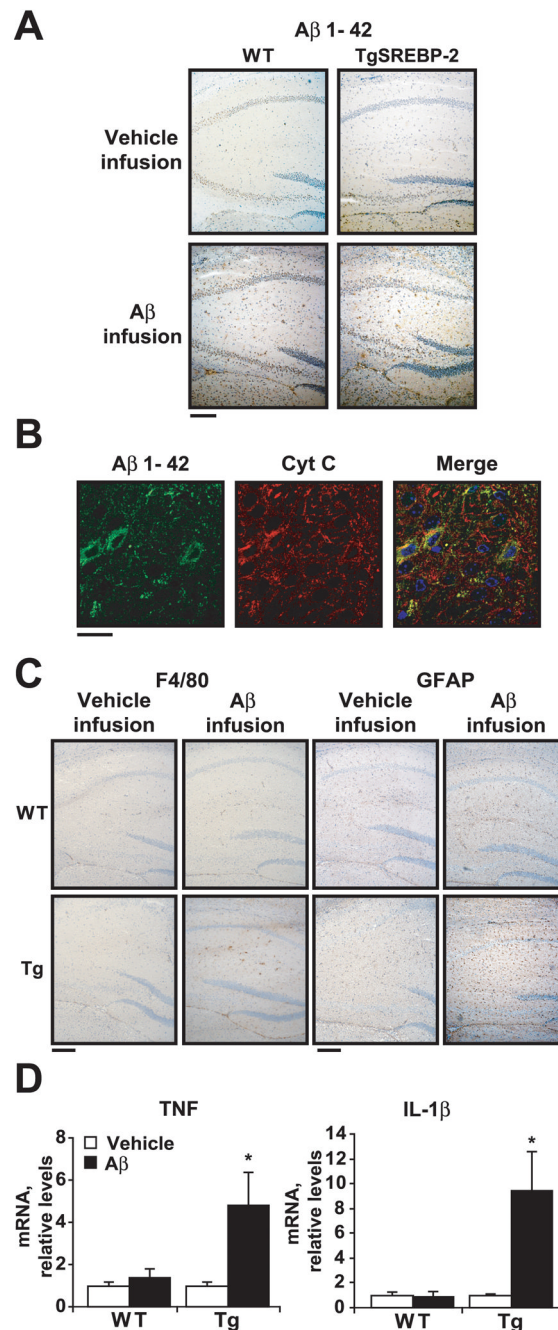
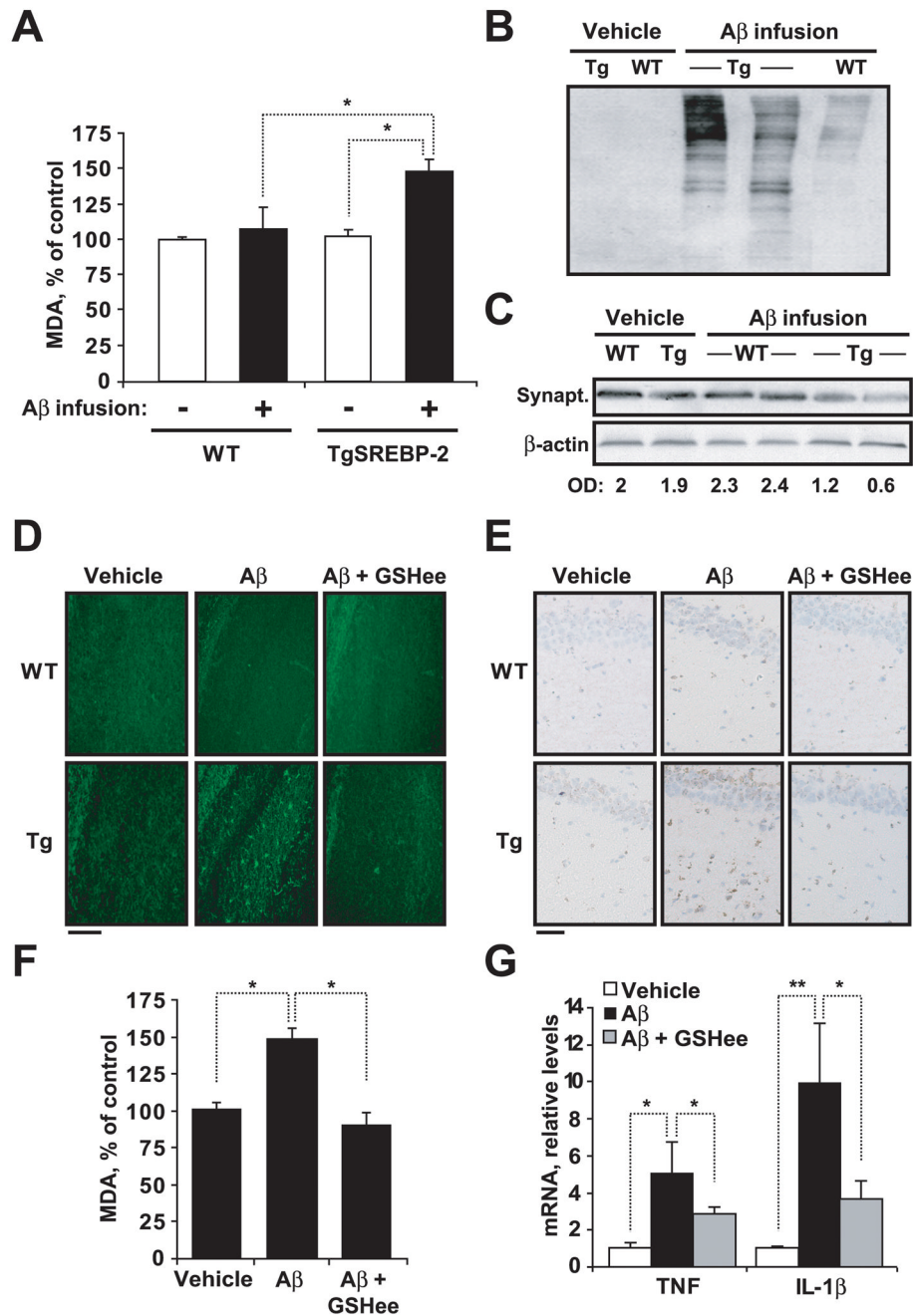


Figure 5. Increased neuroinflammation in SREBP-2 transgenic mice following A β 1-42 infusion. Wild-type (WT) and SREBP-2 transgenic mice were subjected to continuous intracerebroventricular infusion of vehicle or human A β 1-42 solution (1.2 μ g / day) for 28 days; then, half of the brain was processed for immunohistochemistry and the other hemisphere used for biochemical analysis. $n = 6-8$ mice per group. **A**, A β 1-42 immunohistochemical staining. Representative photomicrographs of hippocampus from WT and transgenic mice after infusion are shown. Scale bar: 100 μ m. **B**, Confocal analysis of A β internalisation. Shown are representative images of A β 1-24 (green) and cytochrome c (red) immunofluorescence from hippocampal sections of TgSREBP-2 brains after the infusion period. Merged image indicates partial co-localization

of A β with the mitochondrial marker cytochrome c (yellow). Nuclei were stained with Hoescht-33258 (shown only in merged image; blue). Scale bar: 10 μ m. **C**, Activation of microglia and astrocytes analyzed by F4/80 and GFAP immunostaining, respectively. Shown are representative photomicrographs of F4/80 and GFAP immunoreactivity as indicated, in sections of hippocampus from infused WT and SREBP-2 transgenic mice (Tg). Scale bar: 100 μ m. **D**, TNF- α and IL-1 β mRNA expression analyzed by real-time PCR from WT and SREBP-2 transgenic brain (Tg) after vehicle or A β infusion. Shown are relative values following normalization against 18s expression and are representative of three experiments \pm S.D. * P < 0.01 vs. vehicle-infused TgSREBP-2 mice. Mean differences were compared by unpaired Student's t test.

**Figure 6.**

A β -infused TgSREBP-2 mice display enhanced oxidative stress and neuronal damage which is prevented by GSH ethyl ester (GSHee) co-infusion. Wild-type (WT) and TgSREBP-2 mice were subjected to continuous infusion of vehicle or human A β 1-42 solution (1.2 μ g / day) for 28 days. $n = 6-8$ mice per group. **A**, Lipid peroxidation estimated as production of malondialdehyde (MDA). * $P < 0.03$. **B**, Representative immunoblotting showing presence of carbonyl proteins in WT and TgSREBP-2 (Tg) brains following infusion. **C**, Representative immunoblotting showing synaptophysin protein levels after infusion. Densitometric values of the bands representing synaptophysin immunoreactivity were normalized with the values of the corresponding β -actin bands (O.D.: normalized optical density). **D**, Representative images

of degenerated neurons in hippocampal regions by Fluoro-Jade B staining. Scale bar: 50 μm . **E**, Representative images of apoptotic cells in hippocampus by terminal deoxynucleotidyl transferase-mediated nick-end labeling (TUNEL). Scale bar: 25 μm . **F**, Lipid peroxidation in infused TgSREBP-2 brains estimated as malondialdehyde levels (MDA). * $P < 0.01$ ($n = 6$). **G**, TNF- α and IL-1 β mRNA expression analyzed by real-time PCR from infused TgSREBP-2 brains. Relative values were normalized against 18s expression. * $P < 0.05$, ** $P < 0.01$ ($n = 6$). Values are mean \pm S.D.; mean differences were compared by unpaired Student's t test.

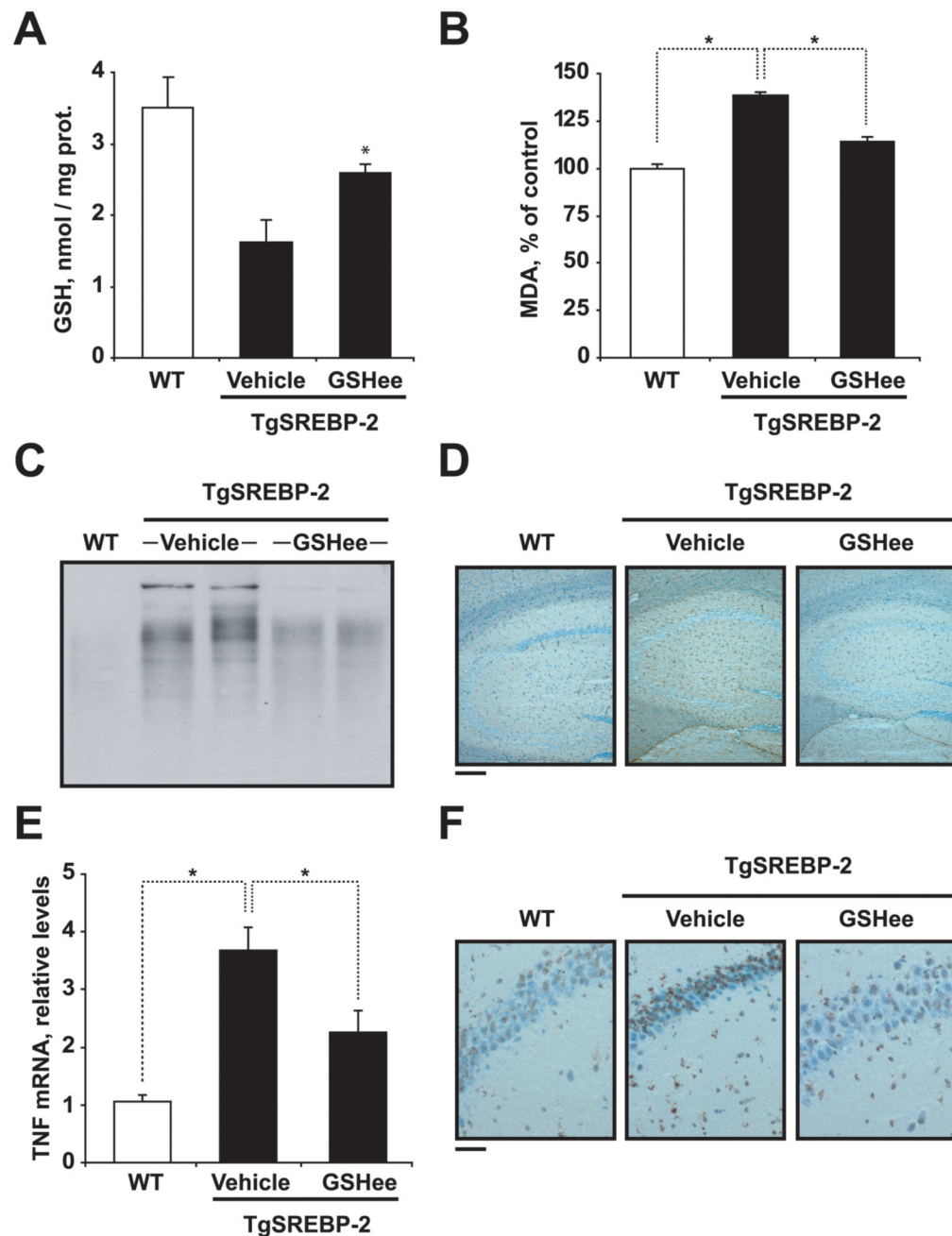
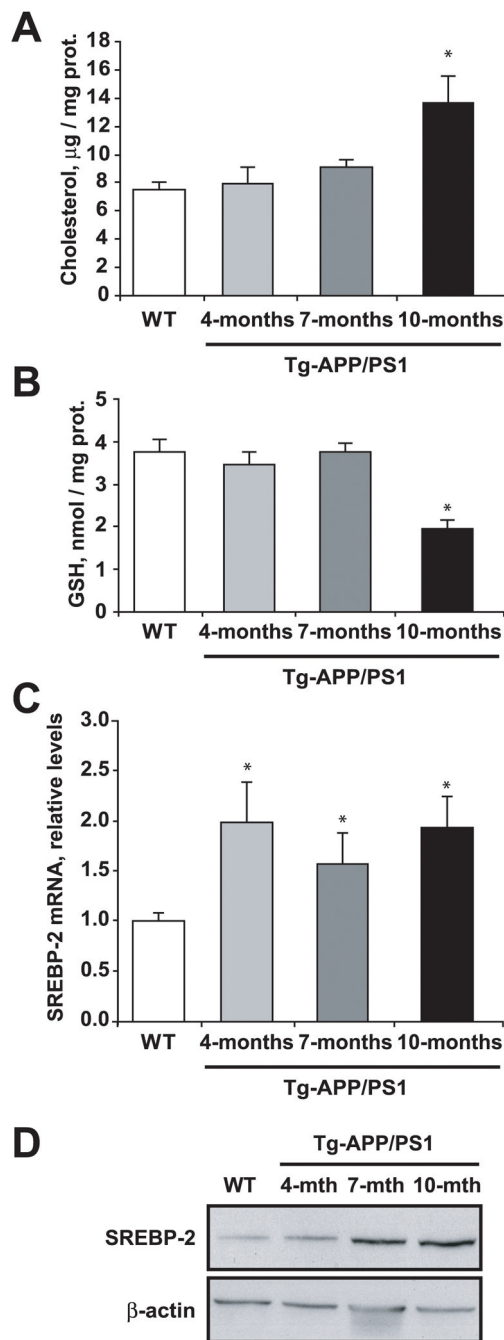


Figure 7. GSH ethyl ester (GSHee) i.p. therapy protects against A β -induced neurodegeneration in TgSREBP-2 mice. Wild-type (WT) and TgSREBP-2 mice were subjected to continuous infusion of human A β 1-42 solution (1.2 μ g / day) for 28 days. GSH ethyl ester (1.25 mmol / Kg / day) or vehicle alone were administered i.p. over the last two week of the infusion period. $n = 4-6$ mice per group. **A**, Mitochondrial GSH levels. * $P = 0.01$. **B**, Lipid peroxidation estimated as production of malondialdehyde (MDA). * $P < 0.01$. **C**, Representative immunoblotting showing presence of carbonyl proteins. **D**, Activation of astrocytes analyzed by GFAP immunostaining. Shown are representative photomicrographs GFAP immunoreactivity in hippocampal sections. Scale bar: 100 μ m. **E**, TNF- α expression analyzed by real-time PCR. Relative values were

normalized against 18s expression. * $P < 0.05$. *F*, Representative images of apoptotic cells in hippocampus by terminal deoxynucleotidyl transferase-mediated nick-end labeling (TUNEL). Scale bar: 25 μm . Values are mean \pm S.D.; mean differences were compared by unpaired Student's t test.

**Figure 8.**

Brain mitochondria from 10-months old AD transgenic mice exhibit increased cholesterol and depleted GSH levels. **A**, Total cholesterol levels and **B**, GSH levels of isolated brain mitochondria from 10-months old WT mice and AD transgenic mice (Tg-APP/PS1) at the indicated ages. $*P < 0.05$ ($n = 3-4$). **C** and **D**, SREBP-2 expression in brain extracts from 10-months old WT mice and Tg-APP/PS1 transgenic mice at the indicated ages. **C**, SREBP-2 mRNA expression analyzed by real-time PCR. Relative values were normalized against 18s expression. $*P < 0.05$ ($n = 3-4$). **D**, Representative immunoblotting showing SREBP-2 protein levels. β -Actin levels were analyzed as a loading control. Values are mean \pm S.D.; mean differences were compared by unpaired Student's t test.